

Research Article

Nonparametric Interference Suppression Using Cyclic Wiener Filtering: Pulse Shape Design and Performance Evaluation

Anass Benjebbour, Takahiro Asai, and Hitoshi Yoshino

Research Laboratories, NTT DoCoMo, Inc., 3-5 Hikarinooka, Yokosuka, Kanagawa 239-8536, Japan

Correspondence should be addressed to Anass Benjebbour, anass@nttdocomo.co.jp

Received 29 June 2007; Accepted 23 October 2007

Recommended by Ivan Cosovic

In the future, there will be a growing need for more flexible but efficient utilization of radio resources. Increased flexibility in radio transmission, however, yields a higher likelihood of interference owing to limited coordination among users. In this paper, we address the problem of flexible spectrum sharing where a wideband single carrier modulated signal is spectrally overlapped by unknown narrowband interference (NBI) and where a cyclic Wiener filter is utilized for nonparametric NBI suppression at the receiver. The pulse shape design for the wideband signal is investigated to improve the NBI suppression capability of cyclic Wiener filtering. Specifically, two pulse shaping schemes, which outperform existing raised cosine pulse shaping schemes even for the same amount of excess bandwidth, are proposed. Based on computer simulation, the interference suppression capability of cyclic Wiener filtering is evaluated for both the proposed and existing pulse shaping schemes under several interference conditions and over both AWGN and Rayleigh fading channels.

Copyright © 2008 Anass Benjebbour et al. This is an open access article distributed under the Creative Commons Attribution License, which permits unrestricted use, distribution, and reproduction in any medium, provided the original work is properly cited.

1. INTRODUCTION

In future wireless systems, there is a need to support the explosive growth in number of users, be they persons or machines, and the ever-increasing diversity in wireless applications and user requirements. Nevertheless, one of the most challenging issues is the need to maximize the utilization of scarce radio resources. In recent years, as a solution towards a more efficient, yet flexible usage of spectrum resources, opportunistic overlay sharing of underutilized, already assigned spectrum has been under consideration [1, 2]. Design flexibility in radio, however, entails several challenging technical problems because of the eventual interference owing to limited coordination between multiple users of possibly heterogeneous transmission characteristics, for example, symbol rate, symbol timing, carrier frequency, and modulation scheme. Thus, with the aim of achieving a higher degree of flexibility in spectrum usage, the development of nonparametric interference suppression/avoidance techniques to deal with heterogeneous unknown in-band interference is regarded as a crucial issue. In previous studies, interference suppression/avoidance techniques for orthogonal frequency division multiplexing- (OFDM-) based systems were investi-

gated [3, 4]. In this paper, a spectrum sharing scenario where a wideband single carrier modulated signal is jammed by unknown NBI is investigated and a cyclic Wiener (CW) filter is utilized to take advantage of the property of cyclostationarity for nonparametric NBI suppression.

A signal is said to exhibit cyclostationarity if its cyclic autocorrelation function is nonzero for a nonzero cycle frequency. Single carrier modulated signals are known to exhibit cyclostationarity and so are said to be cyclostationary [5, 6]. Cyclostationarity-exploiting signal processing algorithms are known to outperform classical algorithms, that is, algorithms that have been designed assuming a stationary model for all the signals involved in the reception problem. The utilization of cyclostationarity in signal processing has been studied from several aspects, for example, blind channel estimation, equalization, and direction estimation in adaptive array antennas [7–10]. For nonparametric interference suppression, early studies and proposals on utilizing cyclostationarity using CW filtering were established in [6, 11, 12]. Compared to classical Wiener filters optimized against only the presence of additive white Gaussian noise (AWGN), CW filters are shown to be able to better suppress cochannel interference [6, 13–16]. In [13], for example, the CW filter is

shown to be effective in suppressing NBI in CDMA systems, where the cyclostationarity of the NBI is utilized after estimating its corresponding cycle frequencies. Nevertheless, in a flexible spectrum usage environment, with limited coordination it is not always possible to rely on the cyclostationarity property of the NBI, for example, the case when the NBI does not exhibit sufficient cyclostationarity to be utilized. Other papers that perform blind source separation (BSS) based on cyclostationarity also include [17, 18]. However, interference suppression in these papers utilizes spatial filtering by assuming multiple antennas at the receiver. In this paper, we focus mainly on the exploitation of the spectral structure owing to the cyclostationarity property of the wideband signal. The NBI is assumed stationary and the exploitation of the spatial structure by multiple antennas at the receiver is left as optional.

The interference suppression capability of a CW filter is proportional to the amount of cyclostationarity available. For a single carrier modulated signal, the amount of cyclostationarity is strongly related to the spectral structure of the signal, represented by the cyclic nature of its second-order statistics, which itself is related to the pulse shaping filter used for limiting its occupied spectrum. In the context of crosstalk suppression, a near-optimal solution for transmit pulse shaping is derived to maximize the usage of cyclostationarity [19, 20]. Unfortunately, this solution, besides being computationally intensive, is impractical in our scenario as it is dependent on the channel impulse response of NBI and also the signal-to-noise ratio (SNR) value. On the other hand, other existing raised cosine pulse shaping schemes are designed to satisfy the Nyquist criterion of zero intersymbol interference (ISI) to reduce self-interference; however, they do not take the existence of external interference into consideration and they are widely used for excess bandwidths of less than 100%, that is, a roll-off factor of less than 1.0. To improve the CW capability to suppress the external in-band interference, a larger amount of cyclostationarity needs to be induced by expanding the excess bandwidth of the existing pulse shaping schemes. For this purpose, raised cosine pulses derived for excess bandwidths beyond 100% can be utilized [21, 22]. However, it is not clear to what extent the interference suppression capability of CW filtering can be enhanced using such pulse shaping.

1.1. Contributions

The objective of this work is to clarify the impact of pulse shaping design on the interference suppression capability of CW filtering. Specifically, we propose for a wideband signal, for both the cases of unknown and known carrier frequency offsets (CFOs), two new pulse shaping schemes that outperform existing raised cosine pulse shaping schemes even for the same amount of excess bandwidth. Based on computer simulation, the performance of CW filtering is evaluated under several interference conditions and over both AWGN and Rayleigh fading channels. With regard to the impact of pulse shaping on the interference suppression capability of CW filtering, simulation results reveal that there is no advantage derived from increasing the excess bandwidth of existing pulse

shaping for the case of NBI with a large CFO, that is, NBI lying outside the Nyquist bandwidth of the wideband signal. Also, the results show that for the case of NBI with a small unknown or known CFO, the proposed pulse shaping schemes, compared to existing pulse shaping schemes, yield (1) substantially improved quality of extraction for the wideband signal; and (2) less interference from the wideband signal-to-narrowband signal.

The remainder of this paper is structured as follows. Section 2 introduces the fundamentals of cyclostationarity and CW filtering. Section 3 presents the assumed signal model and basic receiver structure. In Section 4 after a brief review of near-optimal and existing pulse shaping schemes, the concept of the proposed pulse shaping is explained and examples are described for both the cases of unknown and known CFO. Section 5 presents extended receiver structures for the narrowband signal, frequency-selective channels, and multiple receive antennas. Simulation results are presented in Section 6. The paper concludes in Section 7 with a summary recapping the main advantages of the proposed pulse shaping schemes.

1.2. Notations

Lower-case bold, as in \mathbf{x} , denotes vectors and $*$ denotes a complex conjugation. Term E represents the probabilistic expectation, $\langle \cdot \rangle$ denotes the average over time, \otimes is the convolution operator, and δ is Dirac's delta function. Given a matrix \mathbf{A} , \mathbf{A}^T represents its transpose, \mathbf{A}^\dagger its Hermite conjugate, and $\|\mathbf{A}\|$ its vector norm.

2. TECHNICAL BACKGROUND

In this section, we briefly review concepts that are related to cyclostationarity and are relevant to this paper.

2.1. Wide-sense cyclostationarity

Let $a(t)$ be a complex-valued zero-mean signal. The signal, $a(t)$, is said to be wide-sense (second-order) cyclostationary or exhibit wide-sense cyclostationarity (WSCS) [5] with cycle frequency, $\gamma \neq 0$, if and only if the Fourier transform of its time dependent autocorrelation function, $R_{aa}(t + \tau/2, t - \tau/2) = E[a(t + \tau/2)a^*(t - \tau/2)]$, called the cyclic autocorrelation function (CAF),

$$R_{aa}^\gamma(\tau) = \lim_{I \rightarrow \infty} \frac{1}{I} \int_{-I/2}^{I/2} R_{aa}\left(t + \frac{\tau}{2}, t - \frac{\tau}{2}\right) e^{-j2\pi\gamma t} dt, \quad (1)$$

is not zero for some values of lag parameter τ . In (1), I is the observation time interval. On the other hand, the signal, $a(t)$, is said to exhibit conjugate WSCS with cycle frequency, $\beta \neq 0$, if and only if the Fourier transform of its conjugate time dependent autocorrelation function, $R_{aa^*}(t + \tau/2, t - \tau/2) = E[a(t + \tau/2)a(t - \tau/2)]$, called the conjugate CAF,

$$R_{aa^*}^\beta(\tau) = \lim_{I \rightarrow \infty} \frac{1}{I} \int_{-I/2}^{I/2} R_{aa^*}\left(t + \frac{\tau}{2}, t - \frac{\tau}{2}\right) e^{-j2\pi\beta t} dt, \quad (2)$$

is not zero for some values of lag parameter τ .

Another essential way of characterizing WSCS and conjugate WSCS stems from the cyclic nature of the power spectrum density of a cyclostationary signal. This is represented by the Fourier transform of CAF, known as spectral correlation density (SCD) and is given by

$$\begin{aligned} S_{aa}^\gamma(f) &= \int_{-\infty}^{\infty} R_{aa}^\gamma(\tau) e^{-j2\pi f\tau} d\tau, \\ &= \lim_{T \rightarrow \infty} T \left\langle A_T \left(t, f + \frac{\gamma}{2} \right) A_T^* \left(t, f - \frac{\gamma}{2} \right) \right\rangle, \end{aligned} \quad (3)$$

where

$$A_T(t, \nu) = \frac{1}{T} \int_{t-T/2}^{t+T/2} a(u) e^{-j2\pi\nu u} du \quad (4)$$

is the complex envelope of the spectral component of $a(t)$ at frequency ν with approximate bandwidth $1/T$. Similarly,

$$\begin{aligned} S_{aa^*}^\beta(f) &= \int_{-\infty}^{\infty} R_{aa^*}^\beta(\tau) e^{-j2\pi f\tau} d\tau \\ &= \lim_{T \rightarrow \infty} T \left\langle A_T \left(t, f + \frac{\beta}{2} \right) A_T \left(t, -f + \frac{\beta}{2} \right) \right\rangle. \end{aligned} \quad (5)$$

Accordingly, the cycle frequencies, γ , correspond to the frequency shifts for which the spectral correlation expressed by (3) is nonzero. Similarly, the cycle frequencies, β , correspond to the frequency shifts for which the conjugate spectral correlation expressed by (5) is nonzero.

Also note that for $\gamma = 0$, the CAF, R_{aa}^γ , reduces to the classical autocorrelation function of $a(t)$. For single carrier modulated signals, the cycle frequencies γ are equal to the baud rate and harmonics thereof. Meanwhile, cycle frequencies β are equal to twice the carrier frequency, possibly plus or minus the baud rate and harmonics thereof. Following this, conjugate cyclostationarity can be observed in carrier-modulated signals [6]. However, the conjugate CAF, $R_{aa^*}^\beta$, reduces to zero for single carrier modulated baseband signals when balanced modulation, for example, quadrature amplitude modulation (QAM), is used.

2.2. CW filtering

It is well known that optimum filters for extracting a signal from a stationary received signal are time-invariant and given by Wiener filters. Similarly, optimum filters for extracting a signal from a received signal that exhibits cyclostationarity with multiple cycle frequencies are multiply-periodic time-variant filters which are shown to be equivalent to frequency shift linear time-invariant filters and are known as CW filters [12]. The general input-output relation of the CW filter for a complex-valued input signal, $a(t)$, is given by

$$d(t) = \sum_{r=1}^R w_r(t) \otimes a_{\gamma_r}(t) + \sum_{s=1}^S v_s(t) \otimes a_{-\beta_s}^*(t), \quad (6)$$

where $a_{\gamma}(t) = a(t)e^{j2\pi\gamma t}$ and $a_{-\beta}^*(t) = a^*(t)e^{j2\pi\beta t}$ are frequency-shifted versions of $a(t)$ and $a^*(t)$, and $d(t)$ is the output signal. Terms R and S are the number of the cycle frequencies γ_r and β_s , respectively. According to (6), the CW filter jointly filters the input signal and its conjugate to produce

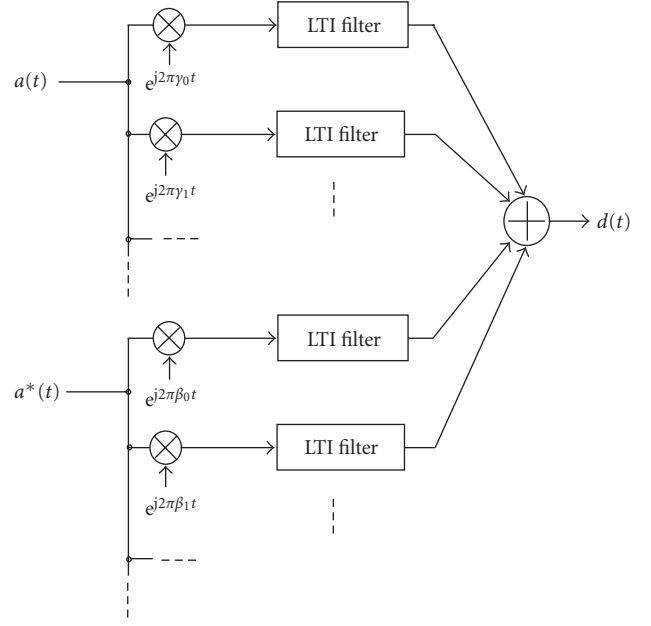


FIGURE 1: Illustration of the general input-output relation for a CW filter.

the output signal. This corresponds to a linear-conjugate-linear (LCL) filter which is optimum for complex-valued signals [23]. Besides, according to (6), the CW filter implicitly utilizes nonconjugate cyclostationarity and conjugate cyclostationarity through R nonconjugate linear time-invariant (LTI) filters of impulse-response, $\{w_r(t)\}$, $r = 1, \dots, R$, and S conjugate LTI filters of impulse response, $\{v_s(t)\}$, $s = 1, \dots, S$, respectively.

Taking the Fourier transforms of both sides of (6), we obtain

$$d(f) = \sum_{r=1}^R W_r(f) A(f - \gamma_r) + \sum_{s=1}^S V_s(f) A^*(-f + \beta_s). \quad (7)$$

From (6) and (7), the input signal and its conjugate are, respectively, subjected to a number of frequency-shifting operations by amount γ_r and β_s , then these are followed by LTI filtering operation with impulse response functions $w_r(\cdot)$ and $v_s(\cdot)$ and transfer functions $W_r(\cdot)$ and $V_s(\cdot)$. Subsequently, a summing operation of the outputs of all LTI filters is performed. As a result, for a cyclostationary input signal, $a(t)$, the CW filter is equipped with the necessary operations to take advantage of the spectral structure of $a(t)$ owing to the nonzero correlation between $A(f)$ and $A^*(f - \gamma)$, and $A(f)$ and $A(-f + \beta)$ (cf. (3) and (5)). An illustration of the general input-output relation of the CW filter is depicted in Figure 1.

3. DESCRIPTION OF ASSUMED SPECTRUM SHARING SCENARIO

In this section, we introduce the assumed spectrum sharing scenario. This is illustrated in Figure 2. The signal model and

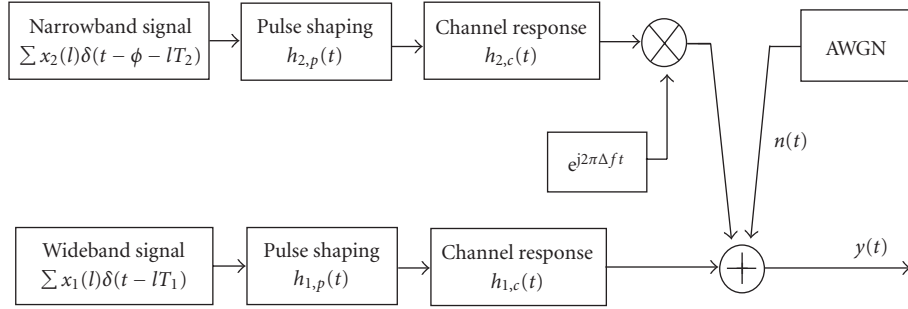


FIGURE 2: Illustration of the baseband signal model of two spectrally overlapping asynchronous signals having different symbol rates and a carrier frequency offset.

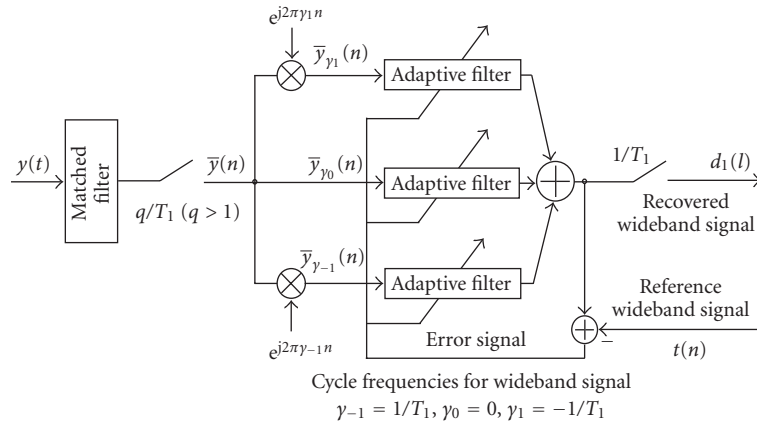


FIGURE 3: The receiver structure CW₁: a matched filter followed by a CW filter that extracts the wideband signal by exploiting the cyclostationarity of the wideband signal.

the basic structure for the receiver used are described in the following.

3.1. Signal model

The assumed signal model consists of one wideband single-carrier modulated signal, one narrowband signal and noise. The complex envelope of the received baseband signal, $y(t)$, is given by

$$y(t) = \sum_l x_1(l)\delta(t - lT_1) \otimes h_{1,p}(t) \otimes h_{1,c}(t) + \left(\sum_l x_2(l)\delta(t - lT_2 - \phi) \otimes h_{2,p}(t) \otimes h_{2,c}(t) \right) \times e^{j2\pi\Delta f t} + n(t). \quad (8)$$

At the right side of (8), the first term corresponds to the wideband signal with a baud rate of $1/T_1$, the second term corresponds to the narrowband signal with a baud rate of $1/T_2 < 1/T_1$, and the last term, $n(t)$, represents complex white circular Gaussian noise. Terms Δf and ϕ are the carrier frequency offset and the symbol timing offset between the wideband and narrowband signals, respectively. In addition, $h_{1,p}(t)$, $h_{2,p}(t)$ and $h_{1,c}(t)$, $h_{2,c}(t)$ are the time response of the transmit pulse shaping filters and the channel impulse

responses for the wideband and narrowband signals, respectively. The transmitted symbols for the wideband and narrowband signals, $x_1(l)$ and $x_2(l)$, are modulated using balanced QAM.

In the signal model above, we assume that only the wideband signal is cyclostationary, that the narrowband signal is stationary, that its parameters are basically unknown to the wideband signal, and that a CW filter is utilized at the receiver for non-parametric suppression of NBI. Then to improve the quality of extraction of the wideband signal using the CW filter described in the previous section, the design of the pulse shaping filter, $h_{1,p}$, is studied. In the next section, we first present in detail the basic structure that is assumed for the CW receiver.

3.2. Basic receiver structure

The basic structure of the CW receiver used is shown in Figure 3. Prior to entering the CW filter, a matched filter is used as a static filter to enhance the SNR. Then, the CW filter serves as a dynamic adaptive filter to minimize the time-averaged mean squared error (TA-MSE) between its output and the reference target signal. Since balanced QAM is used for the wideband signal, only nonconjugate branches are of interest to the CW filter; and having one interferer the number of branches is limited to three, where

each branch corresponds to one cycle frequency, $\gamma \in A = \{-1/T_1, 0, 1/T_1\}$, for the wideband signal. Let us denote the target signal as $t(n)$ and the oversampled received signal as $\bar{y}(n) = y(n/T_s)$, where $T_s = q/T_1$ ($q > 1$) is the sampling rate. This receiver is denoted as CW_1 . The receiver, CW_1 , jointly adjusts the coefficients, \mathbf{W}_γ , of the LTI filters corresponding to nonconjugate branches such that the TA-MSE between the summation of the outputs of the LTI filters and the target signal, $t(n)$, is minimized as follows:

$$\mathbf{W} = \arg \min_{\mathbf{W}} \left[\sum_n E \left[\left\| t(n) - \sum_{\gamma \in A} \mathbf{W}_\gamma^\dagger \otimes \bar{y}_\gamma(n) \right\|^2 \right] \right], \quad (9)$$

where $\mathbf{W} = \{\mathbf{W}_\gamma\}_{\gamma \in A}^T$ and \mathbf{W}_γ and \bar{y}_γ are given by

$$\begin{aligned} \mathbf{W}_\gamma &= [w_\gamma(0) \ w_\gamma(1) \ \cdots \ w_\gamma(L-1)]^T, \\ \bar{y}_\gamma(n) &= [\bar{y}(n-L+1)e^{j2\pi\gamma(n-L+1)} \ \cdots \ \bar{y}(n)e^{j2\pi\gamma n}]^T, \end{aligned} \quad (10)$$

where the LTI filters corresponding to all cycle frequencies, $\gamma \in A$, are fractionally spaced filters of finite impulse response (FIR) of order L .

4. PULSE SHAPE DESIGN

Before transmission a signal is traditionally pulse shaped to limit its occupied bandwidth while still satisfying the Nyquist criterion of zero ISI to reduce self-interference [24]. One of the basic pulses used is the sinc pulse which occupies a minimal amount of bandwidth equal to the Nyquist (i.e., information) bandwidth. The Nyquist bandwidth is given by $[-1/2T_1, 1/2T_1]$ for the wideband signal with a symbol rate of $1/T_1$. However, sinc pulses are noncausal and susceptible to timing jitter; thus, other pulses that occupy more bandwidth than the Nyquist bandwidth are usually employed in practice. The difference between the occupied bandwidth and the Nyquist bandwidth, normalized by the Nyquist bandwidth, is known as the excess bandwidth and measured in percentage. For example, a pulse that occupies twice the Nyquist bandwidth has an excess bandwidth of 100%. Although existing pulse shaping schemes are designed to satisfy the Nyquist criterion of zero ISI, they do not take into account the immunity of the pulse-shaped signal against in-band interference. The optimal pulse shaping that takes advantage of the spectral structure owing to cyclostationarity to suppress in-band interference corresponds to the search for a solution to the joint optimization problem for minimizing the following TA-MSE:

$$\min_{\mathbf{W}, h_{1,p}} \left[\sum_n E \left[\left\| t(n) - \sum_{\gamma \in A} \mathbf{W}_\gamma^\dagger \otimes \bar{y}_\gamma(n) \right\|^2 \right] \right], \quad (11)$$

where $h_{1,p}$ is the impulse response of the transmit pulse shaping filter for the wideband signal and \mathbf{W} is the impulse response of the CW filter at the receiver. The problem of obtaining in closed-form the solution to the above joint optimization is open. One heuristic method to this problem is to

find a near-optimal solution through an iterative alternating search process between the optimal $h_{1,p}$ for a fixed \mathbf{W} and the optimal \mathbf{W} for a fixed $h_{1,p}$ [19, 20]. Nevertheless, this solution involves intensive computation due to large matrix inversion at every iteration until convergence. In addition, and more importantly, this solution turns out to be dependent of the channel impulse response of the NBI and the SNR value, which is not practical for our spectrum sharing scenario with unknown NBI.

4.1. Existing raised cosine pulse shaping

Another possible heuristic solution to the joint optimization problem that requires less complexity consists of minimizing (11) through solely optimizing \mathbf{W} . Thus, $h_{1,p}$ is fixed. Then, for the purpose of obtaining a reduced TA-MSE, a higher amount of cyclostationarity is induced to $h_{1,p}$ by extending its excess bandwidth while still keeping the zero ISI criterion satisfied. Raised cosine pulses, however, are typically obtained for an excess bandwidth up to 100% (i.e., roll-off factor, α , less than 1.0). For excess bandwidths beyond 100%, raised cosine pulses derived in [21, 22] can be deployed. In the following, we describe the frequency responses of existing raised cosine pulses for excess bandwidths less than and beyond 100%:

- (i) raised cosine pulses with excess bandwidth less than 100%:

$$H(f) = \begin{cases} 1, & 0 \leq f \leq \frac{0.5(1-\alpha)}{T_1}, \\ 0.5 \left\{ 1 - \sin \left[\frac{\pi}{\alpha} \left(f - \frac{0.5}{T_1} \right) \right] \right\}, & \frac{0.5(1-\alpha)}{T_1} \leq f \leq \frac{0.5(1+\alpha)}{T_1}, \\ 0, & \frac{0.5(1+\alpha)}{T_1} \leq f, \end{cases} \quad (12)$$

where $H(-f) = H(f)$ and $\alpha \leq 1$ is the roll-off factor of the pulse shaping filter, factor α controls the amount of excess bandwidth;

- (ii) raised cosine pulses with excess bandwidth beyond 100% [21]:

$$H(f) = \begin{cases} \sin \left(\frac{\pi}{2\alpha} \right) \cos \left(\frac{\pi f}{\alpha} \right), & 0 \leq f \leq \frac{0.5(\alpha-1)}{T_1}, \\ 0.5 \left\{ 1 - \sin \left[\frac{\pi}{\alpha} \left(f - \frac{0.5}{T_1} \right) \right] \right\}, & \frac{0.5(\alpha-1)}{T_1} \leq f \leq \frac{0.5(\alpha+1)}{T_1}, \\ 0, & \frac{0.5(\alpha+1)}{T_1} \leq f, \end{cases} \quad (13)$$

where $H(-f) = H(f)$ and $\alpha > 1$.

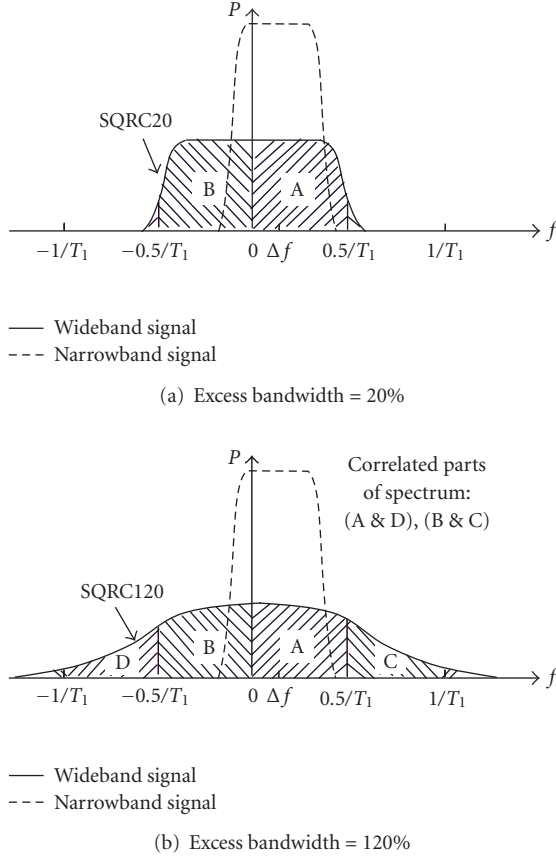


FIGURE 4: Examples of existing raised cosine pulse shaping schemes.

The square root version of existing raised cosine pulses, denoted as SQRC, is given by $\sqrt{H(f)}$ and illustrated in Figure 4 when the excess bandwidth is 20% and 120%.

From the perspective of nonparametric interference suppression using cyclostationarity, one main drawback of the aforementioned existing pulse shaping schemes remains in the manner by which the power is distributed over their frequency response. In fact, most of the power is concentrated around the center carrier frequency within the Nyquist bandwidth, which results in the frequency components outside the Nyquist bandwidth having relatively low power (cf. Figure 4). As will be clarified later in the simulation results, this incurs a very limited interference suppression capability for the CW filter against interference lying within the Nyquist bandwidth of the wideband signal.

4.2. Proposed pulse shaping

For the aforementioned existing pulse shaping schemes, although the excess bandwidth can be increased, this might not always be efficient as it is for the case of interference lying within the Nyquist bandwidth of the wideband signal. Our concern, therefore, is to improve the interference suppression capability of CW filtering while making use of pulse shaping with the minimal amount of excess bandwidth. Here, inspired by ideas from both near-optimal and existing pulse

shaping schemes, we propose a design for pulse shaping, $h_{1,p}$, based on the following two criteria:

- (1) reduce self-interference owing to ISI;
- (2) improve suppression capability against external interference lying within the Nyquist bandwidth of the wideband signal.

Keeping the above two criteria in mind, two pulse shaping schemes are proposed for both the cases of unknown and known CFOs.

4.2.1. Unknown CFO case

For this case, it is not possible to avoid NBI; therefore, the immunity of the wideband signal against NBI must be increased irrespective of the CFO. For this purpose, it is important to design a pulse shaping filter that has a frequency response in which the power is distributed almost uniformly over all the frequency components. As a solution, we propose a time-domain shrunk raised cosine (TSRC) pulse shaping for an excess bandwidth beyond 100%. The frequency response of TSRC pulses is obtained by shrinking the time response, equivalently stretching the frequency response, of the existing raised cosine pulses for excess bandwidth less than 100%. To construct such a pulse for an excess bandwidth $\alpha \times 100\%$ with $m + 1 > \alpha \geq m \geq 1$ (m is a nonzero positive integer), we substitute in (12) α by $(\alpha - m)/(m + 1)$ and f by $f/(m + 1)$. Based on this, the frequency response of a time-domain $1/(m + 1)$ shrunk raised cosine pulse with excess bandwidth $\alpha \times 100\%$ with $m + 1 > \alpha \geq m$ is given by

$$H_{\alpha,m}(f) = \begin{cases} 1, & 0 \leq f \leq \frac{0.5(2m+1-\alpha)}{T_1}, \\ A(f, m), & \frac{0.5(2m+1-\alpha)}{T_1} \leq f \leq \frac{0.5(1+\alpha)}{T_1}, \\ 0, & \frac{0.5(1+\alpha)}{T_1} \leq f, \end{cases}$$

$$A(f, m) = 0.5 \left\{ 1 - \sin \left[\frac{\pi}{(\alpha - m)} \left(fT_1 - \frac{m+1}{2} \right) \right] \right\}, \quad (14)$$

where $H_{\alpha,m}(-f) = H_{\alpha,m}(f)$. In the following, the square root version of these pulses is called time-domain shrunk square root raised cosine, denoted as TSSQRC, and their frequency response is given by $\sqrt{H_{\alpha,m}(f)}$. For $m = 1$, the obtained square root pulses are called time-domain half shrunk square root raised cosine (HSSQRC) pulses. The proposed HSSQRC pulse shaping is illustrated in Figure 5 for an excess bandwidth of 120%.

Regarding the first criterion, it is easy to verify that the TSRC pulses described by (14) satisfy the Nyquist criterion of zero ISI. Regarding the second criterion, TSRC pulse shaping has a lower power concentration compared to the existing raised cosine pulses with the same amount of excess bandwidth. An additional benefit remains in that the power of the frequency components correlated with those within the Nyquist bandwidth is not low anymore; therefore, robustness

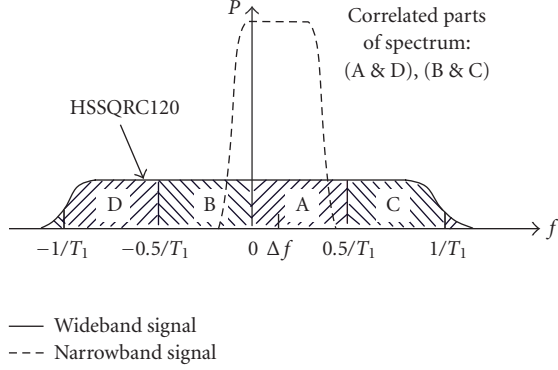
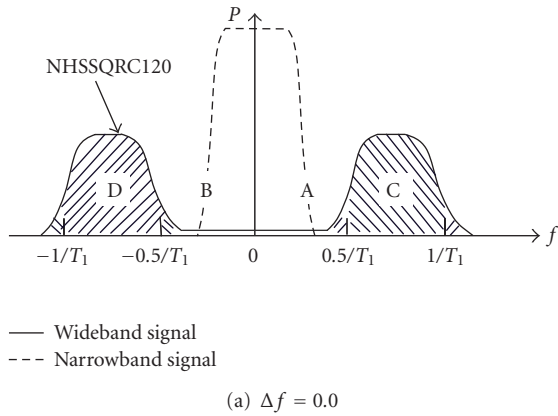
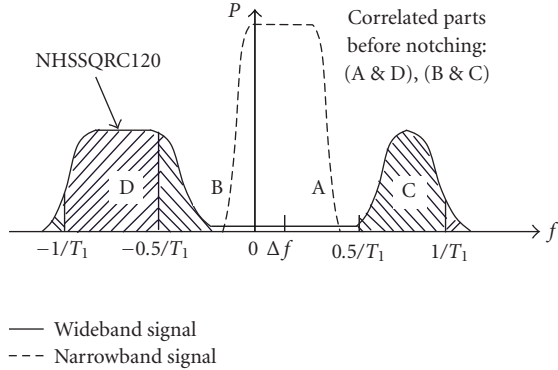


FIGURE 5: An example of proposed pulse shaping for the case of unknown carrier frequency offset.



(a) $\Delta f = 0.0$



(b) $\Delta f = 0.2/T_1$

FIGURE 6: Examples of proposed pulse shaping for the case of known carrier frequency offset.

against interference lying within the Nyquist bandwidth can be expected to increase compared to existing pulse shaping schemes.

4.2.2. Known CFO case

For this case, the knowledge of the CFO can be utilized to minimize interference from the narrowband signal to the wideband signal and concentrate the transmit power of the

wideband signal on spectrum parts that are noncorrupted by the narrowband signal. To make this possible, after increasing the excess bandwidth as in TSRC pulse shaping, we null out (notch) the part of the spectrum inside which the narrowband signal falls. Such a pulse shaping is called notched TSRC (NTSRC).

In the following, we assume that the narrowband signal occupies a bandwidth less than one Nyquist zone ($<1/T_1$) of the wideband signal. This is reasonable because $1/T_2 < 1/T_1$. One smooth construction of NTSRC pulse shaping is obtained by $H_{\alpha,\alpha',\Delta f,m}(f) = H_{\alpha,m}(f) - H_{\alpha',0}(f - \Delta f)$, where one Nyquist zone of the frequency response of the TSRC pulse shaping is nulled out by subtracting the frequency response of a raised cosine pulse having center frequency Δf , a Nyquist bandwidth, $1/T_1$, and an excess bandwidth of $\alpha' \times 100\%$, where $\alpha' < 1$. For $\Delta f = 0$, the frequency response of NTSRC pulse shaping is given by

$$H_{\alpha,\alpha',0,m}(f) = \begin{cases} 0, & 0 \leq f \leq \frac{0.5(1-\alpha')}{T_1}, \\ 1 - A(f, 0), & \frac{0.5(1-\alpha')}{T_1} \leq f \leq \frac{0.5(1+\alpha')}{T_1}, \\ 1, & \frac{0.5(1+\alpha')}{T_1} \leq f \leq \frac{0.5(2m+1-\alpha)}{T_1}, \\ A(f, m), & \frac{0.5(2m+1-\alpha)}{T_1} \leq f \leq \frac{0.5(1+\alpha)}{T_1}, \\ 0, & \frac{0.5(1+\alpha)}{T_1} \leq f, \end{cases} \quad (15)$$

where $H_{\alpha,\alpha',0,m}(-f) = H_{\alpha,\alpha',0,m}(f)$. In the following, the square root version of these pulses is called notched time-domain shrunk square root raised cosine, denoted as NTSSQRC, and their frequency response is given by $\sqrt{H_{\alpha,\alpha',\Delta f,m}(f)}$. For $m = 1$, the obtained square root pulses are called notched time-domain half shrunk square root raised cosine (NHSSQRC) pulses. The proposed NHSSQRC pulse shaping is illustrated in Figure 6 for an excess bandwidth of 120%.

Regarding the first criterion, it is easy to verify that the NTSRC pulse shaping described by (15) does not satisfy the Nyquist criterion of zero ISI. Nevertheless, owing to the properly induced cyclostationarity prior to spectral notching, ISI compensation is feasible by using the CW filter at the receiver. Regarding the second criterion, besides the benefits of the TSRC pulse shaping, for NTSRC pulse shaping, thanks to spectral notching, efficient power allocation is possible as the signal power is not wasted on corrupted spectrum.

5. EXTENDED RECEIVER STRUCTURES

5.1. Receiver for narrowband signal

In a spectrum sharing environment where the narrowband signal is also of interest, it is also important to reveal whether the proposed pulse shaping for the wideband signal is beneficial to the narrowband signal as well. Here, we describe receivers for the narrowband signal for several cases of different

coordination levels between the narrowband and wideband signals: (1) unknown and known CFOs; and (2) unknown and known cycle frequencies of the wideband signal.

- (i) The case of an unknown CFO: for this case, TSSQRC is utilized for the wideband signal as proposed. For the receiver of the narrowband signal, we consider the two cases below.

(a) *The case where the cycle frequencies of the wideband signal are unknown to the receiver of the narrowband signal.* For this case, the narrowband signal has no information on the characteristics of the wideband signal, and the in-band interference caused by the wideband signal cannot be removed from the narrowband signal. Signal extraction can only be carried out using the matched filter for the narrowband signal, hereafter denoted as MF₂.

(b) *The case where the cycle frequencies of the wideband signal are known to the receiver of the narrowband signal.* For this case, the cycle frequencies of the wideband signal are known to the receiver of the narrowband signal. Having this knowledge, the receiver structure, CW₂, illustrated in Figure 7 can be deployed. The receiver, CW₂, for the narrowband signal is intentionally not equipped with a matched filter to allow for large bandwidth reception that also includes the wideband signal. Its CW filter part utilizes the cycle frequencies of the wideband signal so that the spectral structure for the wideband signal is utilized to remove from the narrowband signal the interference owing to the wideband signal.

- (ii) The case of a known CFO: for this case, since NTSSQRC is utilized, the interference from the wideband signal to the narrowband signal is minimal. Therefore, the extraction of the narrowband signal can be carried out by simply using the matched filter, MF₂.

5.2. Receiver for frequency-selective channels

Over frequency-selective channels, multipath delay yields additional channel ISI. For both proposed and existing pulse shaping schemes, channel ISI causes frequency selectivity of the channel that destroys the spectral structure owing to the cyclostationarity induced by the transmit pulse shaping filter of the wideband signal. Therefore, channel ISI results in reducing the NBI suppression capability of the CW receiver. In order to restore the destroyed spectral structure, the CW filter needs to be combined with an equalization scheme to cope with channel ISI. Here, we combine the CW filter with a decision feedback (DF) filter. This combined receiver is denoted as CW₁/DF and its structure is depicted in Figure 8. It is noteworthy that the merit of the receiver, CW₁/DF, is that nonparametric interference suppression and channel ISI equalization can be performed jointly with no information on the NBI. In the receiver, CW₁/DF, the filter weights for the feedforward part consisting of the CW₁ receiver and the

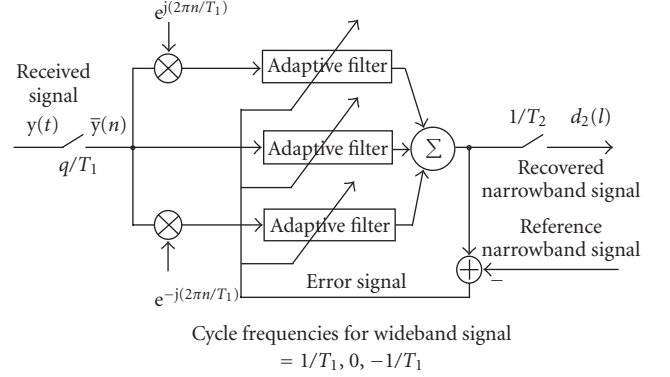


FIGURE 7: The receiver structure CW₂: A CW filter that extracts the narrowband signal by taking advantage of the cyclostationarity of the wideband signal.

filter weights for the feedback part are computed jointly by minimizing the TA-MSE of (16)

$$\mathbf{W} = \arg \min_{\mathbf{W}} \times \left[\sum_l E \left[\left\| t(l) - \left\{ \sum_{y \in A} \mathbf{W}_{f,y}^\dagger \otimes \bar{y}_y(n) \right\}_{l=n/q} - \mathbf{W}_b^\dagger \otimes \tilde{\mathbf{d}}_1(l) \right\|^2 \right] \right]. \quad (16)$$

In (16), $\mathbf{W} = \{ \{ \mathbf{W}_{f,y} \}_{y \in A} \mathbf{W}_b \}^T$ contains the weights for both the feedforward CW and the decision feedback filters. Here, the decision statistic vector, $\tilde{\mathbf{d}}_1$, is given by

$$\tilde{\mathbf{d}}_1(l) = [\tilde{d}_1((l-1)), \tilde{d}_1((l-2)), \dots, \tilde{d}_1((l-L_b))]^T, \quad (17)$$

where the feedback filter is a baud-spaced FIR filter of order L_b .

5.3. Receiver with multiple antennas

When multiple antennas are employed at the receiver, both the spectral and spatial structures of the received signal can be utilized to extract the target signal. This can be achieved by cycle frequency shifting the signals received at all antennas. Thus, the number of branches, that is, LTI filters, for a receiver with N antennas becomes N times the case of a receiver with one single antenna. This receiver is denoted as CW_{1,N} ($N > 1$). The optimization of the weights for all branches is jointly performed for CW_{1,N} as follows:

$$\min_{\mathbf{W}} \left[\sum_n E \left[\left\| t(n) - \sum_{i=1}^N \sum_{y \in A} \mathbf{W}_{iy}^\dagger \otimes \bar{y}_{iy}(n) \right\|^2 \right] \right], \quad (18)$$

where \mathbf{W}_{iy} and \bar{y}_{iy} are given for each receive antenna i similarly to (9).

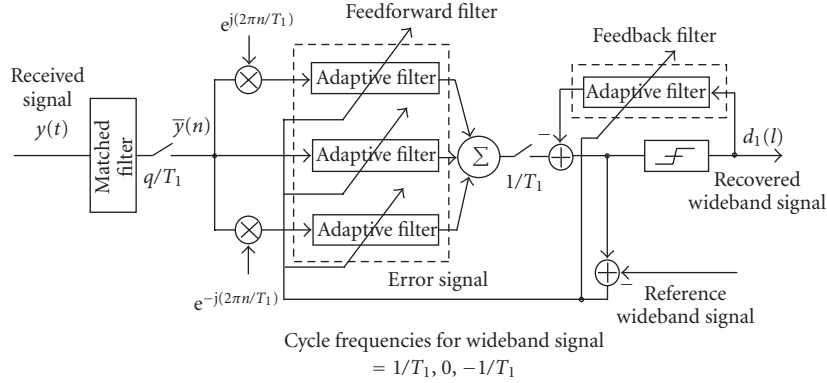


FIGURE 8: The receiver structure CW_1/DF : a CW_1 receiver combined with a decision feedback filter.

6. PERFORMANCE EVALUATIONS

6.1. Computer simulation setup

The bit-error rate (BER) performance of the wideband and narrowband signals is evaluated for the assumed spectrum sharing scenario. The channel models used are AWGN, a frequency-flat Rayleigh fading channel with one single path, and a frequency-selective Rayleigh fading channel with four baud-spaced paths, where the average power ratio between any two successive paths is -4.0 dB. The channel for each path is modeled as quasistatic Rayleigh fading, as we assumed that the channel stays invariant for the whole frame but changes from a frame to another. Basically, the number of antennas N at the receiver is one. If N is more than one, this will be mentioned. Simulation parameters are depicted in Table 1. For the narrowband signal, we use a fixed SQRC pulse shaping with an excess bandwidth of 20% (SQRC20). For the wideband signal, proposed HSSQRC and NHSSQRC pulse shaping schemes are used and compared to existing SQRC pulse shaping schemes, in several channel environments and interference conditions. Throughout all the simulation results, the average received power is normalized to be equal for all proposed HSSQRC, NHSSQRC, and existing SQRC pulse shaping schemes. Also, for NHSSQRC pulse shaping, the factor α' (cf. (15)) is set to 0.2.

6.2. AWGN channel case

BER versus E_b/N_0 for the wideband signal: W/o NBI

In Figure 9, without NBI, the receiver, CW_1 , shows almost the same performance for both existing and proposed pulse shaping schemes regardless of the amount of excess bandwidth. This is because the average received power was normalized to be the same for all pulse shaping schemes.

BER versus E_b/N_0 for the wideband signal: $\Delta f = 0.0$

In Figure 10, with NBI and $\Delta f = 0.0$, the receiver, CW_1 , is used to extract the wideband signal. The BER performance of the wideband signal is largely degraded for existing SQRC20 pulse shaping since it contains a limited amount of cyclostationarity. On the other hand, our proposed HSSQRC120

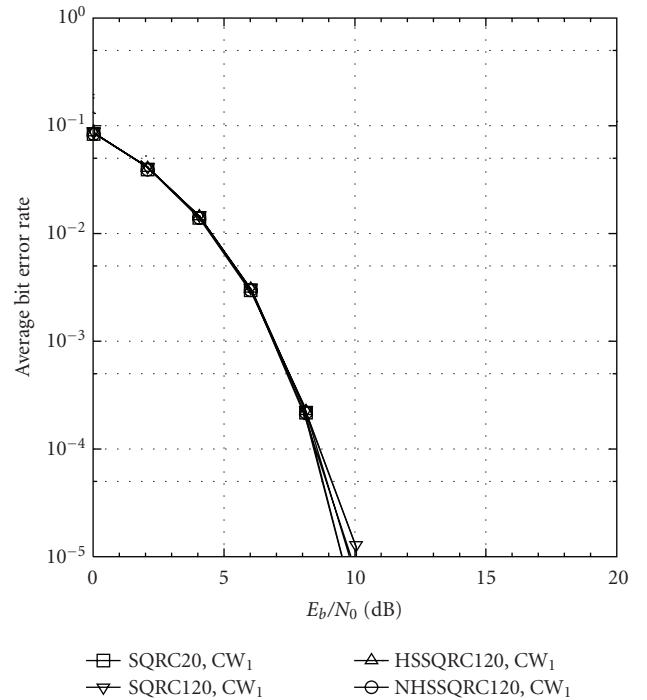


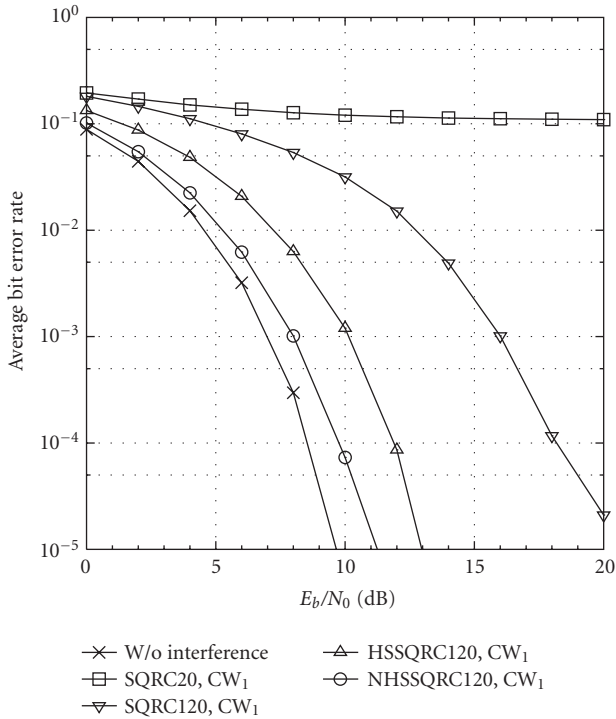
FIGURE 9: BER versus E_b/N_0 for the wideband signal: AWGN channel and w/o NBI.

pulse shaping yields much better BER performance than the existing SQRC120 pulse shaping scheme. This is because less noise enhancement occurs at the CW filter when the HSSQRC and NHSSQRC pulse shaping schemes are used, since the power of the frequency components of the wideband signal separated by one cycle frequency ($\pm 1/T_1$) from its corrupted Nyquist bandwidth is higher with the HSSQRC and NHSSQRC pulses than with the existing SQRC pulses (cf. Figures 4, 5, and 6).

Besides, when the CFO is known to the wideband signal, thus NHSSQRC pulse shaping is used, better performance is achieved compared to HSSQRC pulse shaping. This is because for NHSSQRC pulse shaping, the signal power is not wasted on the corrupted spectrum and is mainly allocated

TABLE 1: Simulation parameters.

Symbol rates	Wideband signal: $1/T_1$, Narrowband signal: $1/T_2 = 1/(2T_1)$
Symbol timing offset	Random, $0 \leq \phi \leq T_1$
Carrier frequency offset	Δf
Power ratio of wideband to narrowband signals	0.0 dB
Channel models	AWGN, one path Rayleigh fading, and exponentially decaying 4-path Rayleigh fading
Modulation scheme	QPSK
Oversampling rate	$4/T_1$ ($q = 4$)
Pulse shaping for narrowband signal	SQRC20 (fixed) Excess bandwidth = 20%
Burst structure (wideband, narrowband)	Training symbols: (128, 64) Information symbols: (512, 256)
Adaptive algorithm	Recursive least squares (RLS) Forgetting factor $\lambda = 1.0$
Number of taps: AWGN/Flat-Rayleigh fading	9 Taps ($L = 9$)
Number of taps: frequency selective fading	33 taps for feedforward filter ($L = 33$), 3 taps for feedback filter ($L_b = 3$)

FIGURE 10: BER versus E_b/N_0 for the wideband signal: AWGN channel and $\Delta f = 0.0$.

to noncorrupted spectrum parts of the wideband signal (cf. Figure 6).

BER versus EBW for the wideband signal:

$\Delta f = 0.0$ and $E_b/N_0 = 10.0$ dB

In Figure 11, the receiver, CW_1 , shows better interference suppression with proposed HSSQRC and NHSSQRC pulses

even for less excess bandwidth (EBW) compared to existing SQRC pulse shaping, for example, HSSQRC with the EBW of 120% versus SQRC with the EBW of 180%. This is because less noise enhancement occurs at the CW filter when proposed pulse shaping is used. On the other hand, an increase in the EBW to beyond 120% does not improve the BER performance for the proposed pulse shaping in Figure 11. This is because the amount of cyclostationarity induced by the proposed pulse shaping for the EBW of almost 120% is already sufficient for suppressing one interferer. A further increase in the EBW simply results in occupying a larger bandwidth, leading to lower power concentration, which degrades the BER performance for the receiver. To exploit the increase in EBW to beyond 120%, the number of branches for receiver, CW_1 , can be increased to more than three; however, the use of more branches comes at the price of more tap weights to estimate and a more complex receiver structure although the BER improvement should be limited with only one interferer.

BER versus Δf for the wideband signal: $E_b/N_0 = 10.0$ dB

In Figure 12, for a relatively large Δf , the receiver, CW_1 , performs sufficiently well with SQRC pulses having a minimal amount of excess bandwidth (e.g., SQRC20). This is because for a relatively large Δf , the matched filter before the CW filter at the receiver, CW_1 , also has a minimal amount of excess bandwidth and consequently can help the CW filter in suppressing interference lying on or outside the boundaries of the bandwidth occupied by the wideband signal. On the other hand, for zero and a small Δf , that is, interference lying within the Nyquist bandwidth of the wideband signal, the receiver, CW_1 , exhibits better performance using the proposed HSSQRC and NHSSQRC pulse shaping schemes. This is because, for a small Δf , the matched filter for existing SQRC pulse shaping cannot suppress the interference. In addition, the CW filter better utilizes the spectral structure owing to

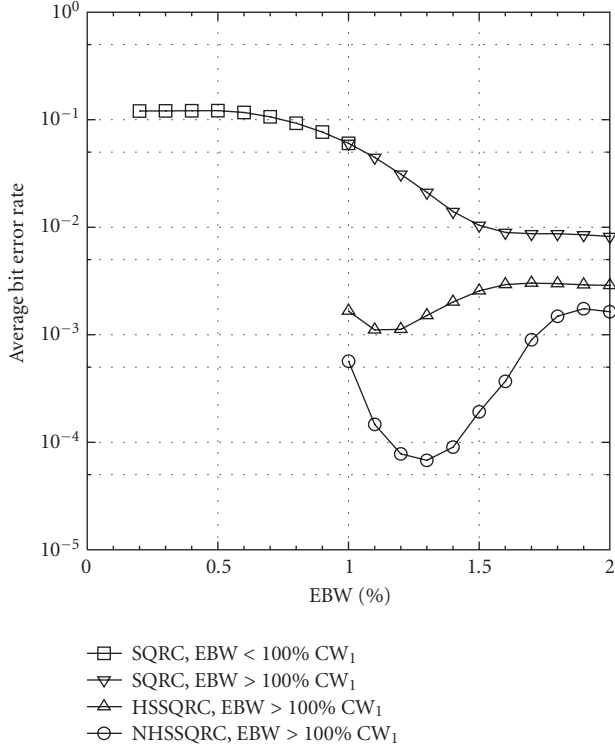


FIGURE 11: BER versus EBW for the wideband signal: AWGN channel, $\Delta f = 0.0$ and $E_b/N_0 = 10.0$ dB.

cyclostationarity for interference suppression with proposed HSSQRC and NHSSQRC pulse shaping compared with existing SQRC pulse shaping. Another important feature is that the BER of the receiver, CW_1 , is kept almost the same irrespective of Δf for the HSSQRC and NHSSQRC pulse shaping schemes. This is brought about by the almost-flat shape of their frequency response (cf. Figures 5 and 6).

BER versus E_b/N_0 for the narrowband signal: $\Delta f = 0.0$

In Figure 13, the BER of the narrowband signal is plotted as a function of E_b/N_0 for $\Delta f = 0.0$. For the narrowband signal, its matched filter, MF_2 , or the receiver, CW_2 , is used as the receiver. For both receivers, HSSQRC and NHSSQRC pulse shaping schemes yield better performance than existing SQRC pulse shaping scheme. When the cycle frequencies of the wideband signal are known to the receiver of the narrowband signal, the narrowband signal can use the receiver, CW_2 , to take advantage of the spectral structure due to the cyclostationarity of the wideband signal to remove its interference from the narrowband signal. For this case as well, the BER performance of the narrowband signal can be improved by using HSSQRC pulse shaping rather than using SQRC pulse shaping. Moreover, when NHSSQRC pulse shaping is used for the wideband signal, the BER performance for the narrowband signal is significantly improved as it receives almost no interference from the wideband signal.

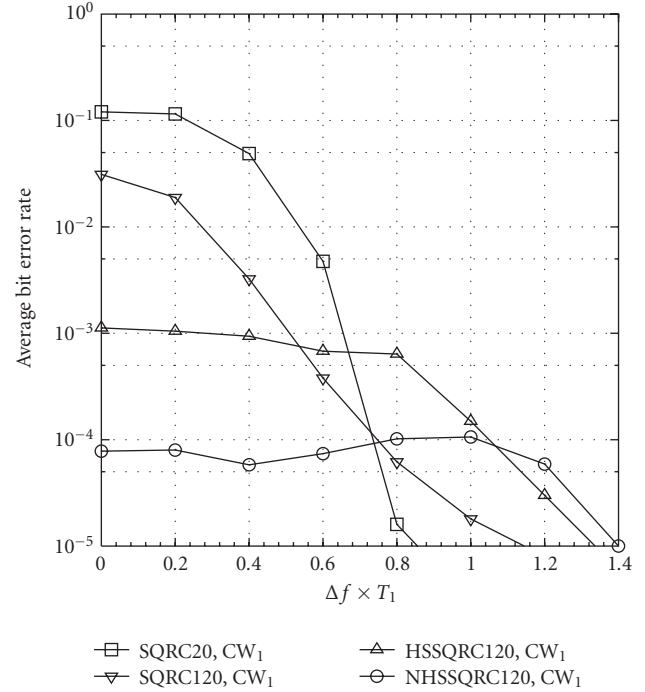


FIGURE 12: BER versus Δf for the wideband signal: AWGN channel and $E_b/N_0 = 10.0$ dB.

6.3. Fading channel case

BER versus E_b/N_0 for the wideband signal: frequency-flat channel, one or two receive antennas, and $\Delta f = 0.0$

In Figures 14 and 15, for both the cases of one receive antenna ($N = 1$) and two receive antennas ($N = 2$), the average BER performance of receivers CW_1 and $CW_{1,2}$ is improved over the frequency-flat fading channel by using pulses with a larger excess bandwidth. Also, for the same excess bandwidth of 120%, the use of HSSQRC120 and NHSSQRC120 pulse shaping schemes results in performance improvement compared to that for SQRC120 pulse shaping. The performance improvement, however, is decreased as N increases. This is because the more spatial degrees of freedom we have for interference suppression, the lower is the noise enhancement effect at the receiver.

BER versus E_b/N_0 for the wideband signal: frequency-selective, one receive antenna and decision feedback equalization, $P = 4$, and $\Delta f = 0.0$

In Figure 16, the average BER versus the average E_b/N_0 for the wideband signal is evaluated over the frequency-selective Rayleigh fading channel. The BER performance for the receiver, CW_1 , is largely degraded. This is because the receiver, CW_1 , fails to equalize the multipath channel when this one is nonminimum phase. Besides, in a frequency-selective channel the receiver, CW_1 , needs to equalize jointly the multipath channel and remove NBI from the received signal. As a result, more degrees of freedom are consumed compared to the case of a frequency-flat channel. Using receiver, CW_1/DF ,

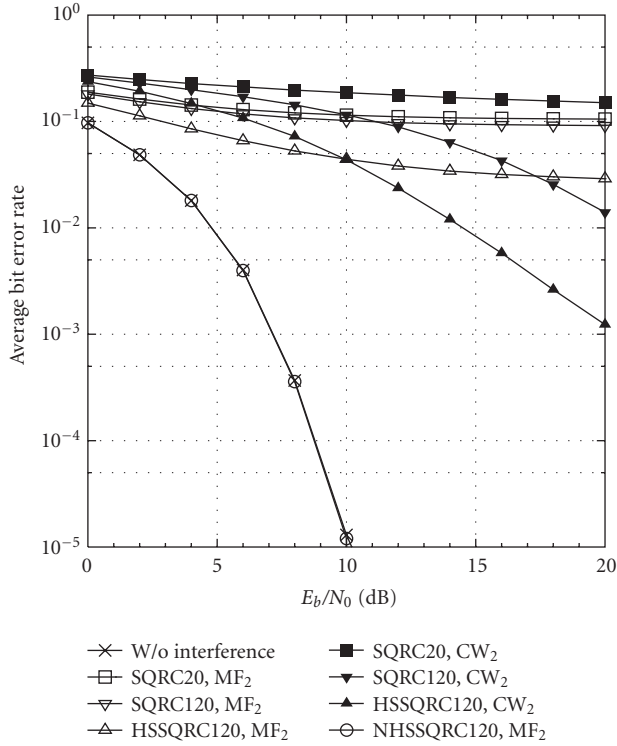


FIGURE 13: BER versus E_b/N_0 for the narrowband signal: AWGN channel and $\Delta f = 0.0$.

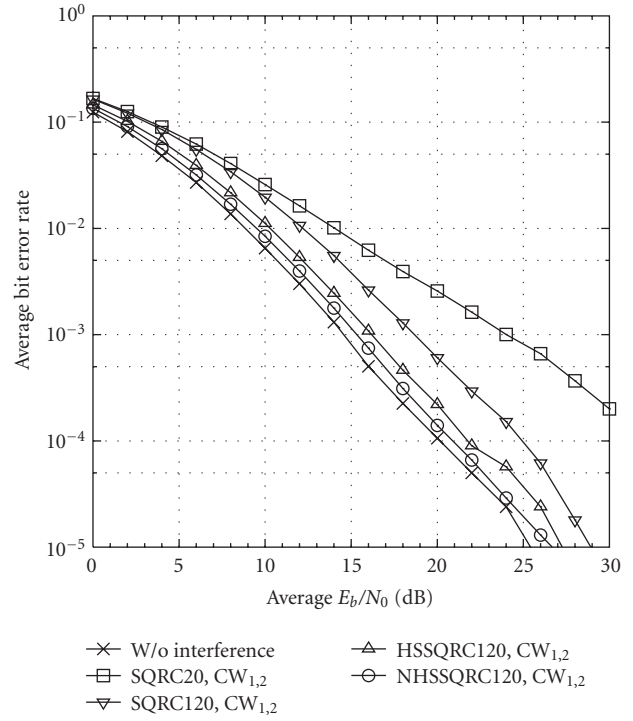


FIGURE 15: BER versus E_b/N_0 for the wideband signal: frequency-flat fading channel, two receive antennas ($N = 2$) and $\Delta f = 0.0$.

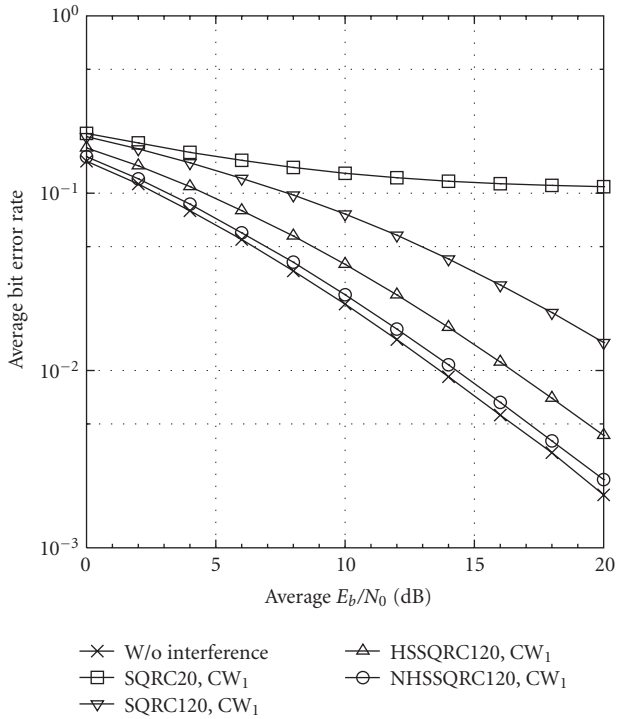


FIGURE 14: BER versus E_b/N_0 for the wideband signal: frequency-flat fading channel, one receive antenna and $\Delta f = 0.0$.

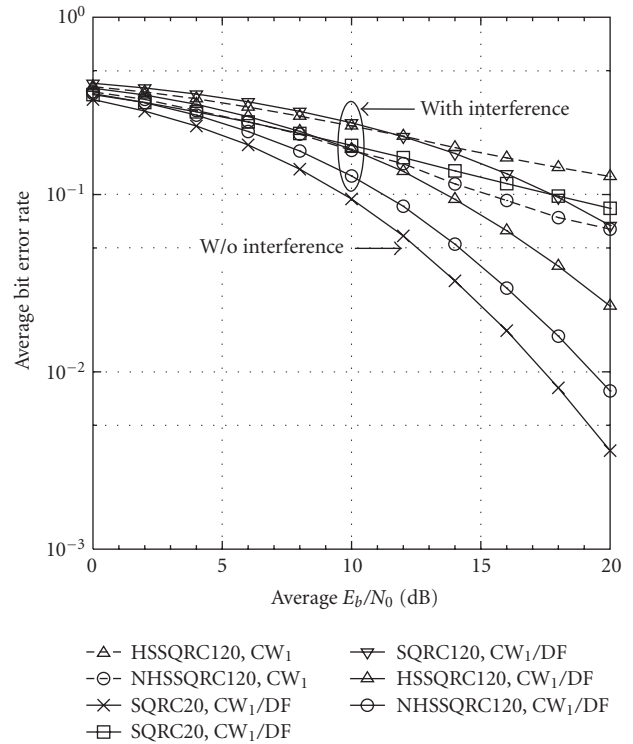


FIGURE 16: BER versus E_b/N_0 for the wideband signal: frequency-selective fading channel, one receive antenna, and $\Delta f = 0.0$.

we obtain a superior performance to that for receiver, CW_1 . Also, a substantial performance improvement is obtained for using the proposed pulse shaping schemes than for using existing pulse shaping schemes. Therefore, by using proposed pulse shaping schemes, the receiver, CW_1/DF , effectively performs joint nonparametric interference and ISI equalization over a frequency selective Rayleigh fading channel, which is disturbed by unknown NBI.

7. CONCLUSION

In this paper, we investigated a flexible spectrum sharing scenario where a wideband single-carrier modulated signal is jammed by unknown NBI. A CW filter is utilized to exploit the cyclostationarity property of the wideband signal for nonparametric suppression of NBI. The impact of pulse shape design on the interference suppression capability of the CW filter is elucidated. For NBI with large CFO, that is, NBI lying outside the Nyquist bandwidth of the wideband signal, we clarified that there is no advantage in modifying the pulse shaping or increasing the excess bandwidth of the pulse shaping filter. For NBI lying within the Nyquist bandwidth of the wideband signal, we proposed new pulse shaping schemes for the wideband signal for both the cases of unknown and known CFOs between the wideband signal and NBI. Through extensive simulation results, we showed that the proposed pulse shaping schemes have the potential to substantially improve the interference suppression capability of CW filtering over both AWGN and Rayleigh fading channels. A large part of the improvement achieved is due to the ability of proposed pulse shaping to take into consideration the existence of interference within the Nyquist bandwidth of the wideband signal by means of increasing their amount of cyclostationarity within a limited amount of excess bandwidth while still minimizing self-interference by reducing ISI. The simulation results also revealed that the proposed pulse shaping performs well over frequency selective channels and for receivers with multiple receive antennas, and is also beneficial to the narrowband signal.

ACKNOWLEDGMENT

This paper was presented in part at the IEEE Vehicular Technology Conference Fall and the IEEE International Symposium on Personal, Indoor, and Mobile Radio Communications, both in September 2006.

REFERENCES

- [1] FCC 2003, "Facilitating opportunities for flexible, efficient, and reliable spectrum use employing cognitive radio technologies," FCC Document ET Docket, no. 03-108, December 2003.
- [2] S. Haykin, "Cognitive radio: brain-empowered wireless communications," *IEEE Journal on Selected Areas in Communications*, vol. 23, no. 2, pp. 201-220, 2005.
- [3] T. Li, W. H. Mow, V. K. N. Lau, M. Siu, R. S. Cheng, and R. D. Murch, "Robust joint interference detection and decoding for OFDM-based cognitive radio systems with unknown interference," *IEEE Journal on Selected Areas in Communications*, vol. 25, no. 3, pp. 566-575, 2007.
- [4] S. Vogeler, L. Broetje, K.-D. Kammeyer, R. Rueckriem, and S. Fechtel, "Blind Bluetooth interference detection and suppression for OFDM transmission in the ISM band," in *Proceedings of the 37th Asilomar Conference on Signals, Systems and Computers (ACSSC '03)*, vol. 1, pp. 703-707, Pacific Grove, Calif, USA, November 2003.
- [5] W. A. Gardner, Ed., *Cyclostationarity in Communications and Signal Processing*, IEEE Press, New York, NY, USA, 1994.
- [6] W. A. Gardner, "Cyclic Wiener filtering: theory and method," *IEEE Transactions on Communications*, vol. 41, no. 1, pp. 151-163, 1993.
- [7] E. Serpedin, F. Panduru, I. Sari, and G. B. Giannakis, "Bibliography on cyclostationarity," *Signal Processing*, vol. 85, no. 12, pp. 2233-2303, 2005.
- [8] D. T. M. Slock and C. B. Papadias, "Blind fractionally-spaced equalization based on cyclostationarity," in *Proceedings of the 44th IEEE Vehicular Technology Conference (VTC '94)*, vol. 2, pp. 1286-1290, Stockholm, Sweden, June 1994.
- [9] A. Chevreuil and P. Loubaton, "Blind second-order identification of FIR channels: forced cyclostationarity and structured subspace method," *IEEE Signal Processing Letters*, vol. 4, no. 7, pp. 204-206, 1997.
- [10] B. G. Agee, S. V. Schell, and W. A. Gardner, "Spectral self-coherence restoral: a new approach to blind adaptive signal extraction using antenna arrays," *Proceedings of the IEEE*, vol. 78, no. 4, pp. 753-767, 1990.
- [11] W. A. Gardner and W. A. Brown, "Frequency-shift filtering theory for adaptive co-channel interference removal," in *Proceedings of the 23rd Asilomar Conference on Signals, Systems and Computers (ACSSC '89)*, vol. 2, pp. 562-567, Pacific Grove, Calif, USA, November 1989.
- [12] E. Ferrara Jr., "Frequency-domain implementation of periodically time-varying filters," *IEEE Transactions on Acoustics, Speech, and Signal Processing*, vol. 33, no. 4, pp. 883-892, 1985.
- [13] G. Gelli, L. Paura, and A. M. Tulino, "Cyclostationarity-based filtering for narrowband interference suppression in direct-sequence spread-spectrum systems," *IEEE Journal on Selected Areas in Communications*, vol. 16, no. 9, pp. 1747-1755, 1998.
- [14] G. Latouche, D. Pirez, and P. Vila, "MMSE cyclic equalization," in *Proceedings of the IEEE Military Communications Conference (MILCOM '98)*, vol. 1, pp. 150-154, Boston, Mass, USA, October 1998.
- [15] J. Zhang, K. M. Wong, Z. Q. Luo, and P. C. Ching, "Blind adaptive FRESH filtering for signal extraction," *IEEE Transactions on Signal Processing*, vol. 47, no. 5, pp. 1397-1402, 1999.
- [16] G. Gelli, L. Paura, and L. Verdoliva, "Adaptive interference suppression in CDMA systems by LCL-PTV filtering," in *Proceedings of the IEEE European Signal Processing Conference (EUSIPCO '00)*, pp. 287-291, Tampere, Finland, September 2000.
- [17] K. Abed-Meraim, Y. Xiang, J. H. Manton, and Y. Hua, "Blind source separation using second-order cyclostationary statistics," *IEEE Transactions on Signal Processing*, vol. 49, no. 4, pp. 694-701, 2001.
- [18] Y.-C. Liang, A. R. Leyman, and B.-H. Soong, "Blind source separation using second-order cyclic-statistics," in *Proceedings of the 1st IEEE Signal Processing Workshop on Signal Processing Advances in Wireless Communications (SPAWC '97)*, pp. 57-60, Paris, France, April 1997.
- [19] G. D. Golden, J. E. Mazo, and J. Salz, "Transmitter design for data transmission in the presence of a data-like interferer," *IEEE Transactions on Communications*, vol. 43, no. 2, part 2, pp. 837-850, 1995.

- [20] M. L. Honig, P. Crespo, and K. Steiglitz, "Suppression of near- and far-end crosstalk by linear pre- and post-filtering," *IEEE Journal on Selected Areas in Communications*, vol. 10, no. 3, pp. 614–629, 1992.
- [21] L. F. Lind, S. G. Methley, and E. Deliot, "Raised cosine filters beyond 100% excess bandwidth," *Electronics Letters*, vol. 31, no. 11, pp. 859–860, 1995.
- [22] L. F. Lind, B.M. Al-Hashimi, and W. P. Somerset, "Linear programming design of FIR raised cosine filters with >100% excess bandwidth," *Electronics Letters*, vol. 32, no. 5, pp. 436–437, 1996.
- [23] W. Brown and R. Crane, "Conjugate linear filtering," *IEEE Transactions on Information Theory*, vol. 15, no. 4, pp. 462–465, 1969.
- [24] J. G. Proakis, *Digital Communications*, McGraw-Hill, Boston, Mass, USA, 4th edition, 2001.